RESEARCH ARTICLE

The relationship between atmospheric blocking and temperature anomalies in Turkey between 1977 and 2016

Bahtiyar Efe[1,2] | İsmail Sezen[1] | Anthony R. Lupo[2] | Ali Deniz[1]

[1]Department of Meteorology, İstanbul Technical University, İstanbul, Turkey

[2]Atmospheric Sciences Program, University of Missouri, Columbia, Missouri

Correspondence
Bahtiyar Efe, İstanbul Technical University, Faculty of Aeronautics and Astronautics, Department of Meteorology, Maslak, 34469 İstanbul, Turkey.
Email: efeba@itu.edu.tr

Abstract

The relationship between the character of atmospheric blocking and surface temperature has not been studied in depth for Turkey. Here, these relationships are investigated for the period 1977–2016. The seasonal mean temperature anomalies for all stations during blocked days varies between −2.1 and 0.8°C. There are four main patterns representing the mean seasonal temperature anomalies for all stations during blocked and non-blocked days. The annual cycle for each group is nearly opposite, and this indicates the impact of blocking on observed temperature, as blocked days comprised 30% of the study period. When focusing on the spatial distribution of mean seasonal anomalies, the winter and fall seasons show that, almost all stations have negative temperature anomalies although anomalies are close to zero during warm seasons (spring and summer). The composite analysis shows that the western part of the country is strongly affected by cold air advection during upstream blocking events and the eastern part of the country is affected by warm temperature advection for downstream blocking events. There is a statistically significant (95% confidence level) negative correlation between blocking intensity and temperature anomalies in all seasons except spring. There is no relationship between both blocking duration and longitudinal extent and the seasonal mean temperature anomaly except during winter, which has a significant negative correlation. The temperature anomaly distribution stratified by season shows that strong positive anomalies are rarely observed in all seasons. Only winter and spring were associated with very strong positive anomalies and only at a few stations. Rex-type atmospheric blocking events are observed during the period of not only the maximum temperature anomaly but also for minimum anomalies. However, the location of the blocking event differed from the typical situation above, with the cold and warm events being located downstream and upstream of Turkey, respectively.

KEYWORDS
atmospheric blocking, climatic seasons, temperature anomalies, Turkey

1 | INTRODUCTION

Atmospheric blocking is a large-scale phenomenon that can be described as the transition between zonal and meridional flow. It has been examined by researchers using different approaches (dynamic, climatological) and including, not only the regional effects, but also remote impacts. These studies focus on the climatological features of atmospheric

blocking (Lupo and Smith, 1995; Tibaldi *et al.*, 1997; Wiedenmann *et al.*, 2002; Barriopedro *et al.*, 2006; Cheung *et al.*, 2013; Dunn-Sigouin *et al.*, 2013), the algorithms for detecting blocking or defining its characteristics (Lejenäs and Økland, 1983; Tibaldi and Molteni, 1990 [*hereafter TM90*]; Lupo and Smith, 1995; Barriopedro *et al.*, 2006), the predictability of atmospheric blocking (TM90; Pavan *et al.*, 2000; Jensen *et al.*, 2017) or the influence of blocking on climatological variables (Antokhina *et al.*, 2016; Whan *et al.*, 2016; Nunes *et al.*, 2017; Sitnov *et al.*, 2017).

The influence of atmospheric blocking on observed regional surface temperature is widely investigated because temperature is a variable of interest to the general public. Diao *et al.* (2015) demonstrated that Eastern Atlantic blocking accompanies frequent cold extremes in Europe. Diao *et al.* (2015) argue that not only does local cooling occur upstream and downstream of the blocking event, but also increased surface air temperatures are the result of atmospheric blocking where they reside. The composite maps examined in this study demonstrated that from 4 days to 1 day before block onset, positive anomalies of geopotential height are located over Northern Europe when negative anomalies are located over Southern Europe.

Whan *et al.* (2016) studied the impacts of upstream atmospheric blocking on wintertime minimum extreme temperatures in North America using numerous data sets. They used the blocking frequency (BF) in Northern Pacific Ocean as covariate when investigating the variation in minimum extreme temperatures by utilizing generalized extreme value theory (GEV). Whan *et al.* (2016) determined that blocking has different impacts on local temperature regimes depending on the location and scale of the event and the location parameters of GEV. Rimbu *et al.* (2014) examined the relationship between not only a blocking index but also other large-scale general circulation patterns in association with large winter temperature extremes in Romania. High blocking activity is related to cold air advection and low blocking activity is related to warm air advection in Romania. Brunner *et al.* (2017) examined the linkage between atmospheric blocking events and European extreme temperatures during the spring season by using E-Obs temperature data set. They found that blocking occurring over central Europe is correlated with warmer conditions while blocking located over the Atlantic and Scandinavia is associated with the cold spells.

Antokhina *et al.* (2018) investigated the effect of atmospheric blocking on surface temperature anomalies for western Siberia during the period from 2004 to 2016. They detected 14 events located over western Siberia and divided these blocking events into two groups. For the first group (10 events), the surface temperature anomalies show a dipole pattern: north(south) of the domain observed positive (negative) anomalies or no temperature anomalies. The second group (four events) was non-dipole.

Sousa *et al.* (2017) investigated the maximum temperature (TX) and minimum temperature (TN) variations in Europe during the period 1948–2012 for both blocking and transient ridge situations. The composite TX, TN temperature anomalies during winter and summer for both blocking and ridge conditions with respect to European regions were obtained. In winter it was shown that during blocking episodes negative anomalies were observed for both TX and TN, but not for ridge events. In contrast, positive TX and TN anomalies observed during ridge situations. During the summer, there was not an opposite signature for blocking and ridge conditions.

Sillmann *et al.* (2011) investigated the influence of North Atlantic Blocking on 2 m minimum temperatures, not only in the re-analysis data (ERA-40) but also for 20th century and future simulations (ECHAM5/MPI-OM, Max Planck Institute for Meteorology in Hamburg, Germany). According to the distribution of ERA-40 and 20th Century data, the Baltic Sea coast line is a primary area that is influenced by atmospheric blocking. During the winter season, long-lasting atmospheric blocking events are correlated with lower minimum temperatures for the vast majority of Europe.

Luo *et al.* (2015) investigated the December 2013 snowstorm that affected the vast majority of Middle East, including Turkey. Luo *et al.* (2015) related cold air advection into the Middle East that produced snowfall to an omega shaped European blocking event, which is the ideal location for the transport cold air into the Middle East. Yao *et al.* (2016) examined the impacts of the North Atlantic Jet on Middle East snowstorms associated with downstream blocking and a positive North Atlantic Oscillation (NAO) index. Yao *et al.* (2016) concluded that strength of the North Atlantic Jet changes the tilt of the block axis in association with a positive NAO during European dipole blocking events.

Türkeş and Erlat (2009) investigated the relationship between winter mean temperatures and the NAO during the period 1950–2003 within Turkey. Cold temperatures were observed over almost all of the 70 surface stations during the positive phase of NAO, and northeasterly flow dominated the period during cold weather. Conversely, during the negative phase of the NAO, westerly flow persists over Turkey and warm temperature anomalies were observed over the vast majority of the country.

The effects of blocking on surface climatological characteristics within Turkey have not been studied widely. Tayanç *et al.* (1998) is the first study that mentions blocking in association with a blizzard event, investigating one of the most famous blizzards that occurred in Istanbul, Turkey. This event lasted from March 3 to 10, 1987. The cause of the blizzard was a persistent cyclone associated with the block that was located over the Balkan region of Europe. Demirtaş (2017) examined the 2012 winter season which was associated with prolonged cold spells in Europe (including

Turkey) due to an omega shaped blocking event centred over Siberia. The European cold waves persisted for time periods of 2–22 days, and in Turkey anywhere from 4 to 18 days, depending on the location within the country.

In spite of all these studies cited above, none of them focus mainly on the nation of Turkey. Many of these studies limit their scope to the cold season and none of these relate surface temperature anomalies to block intensity (BI). Therefore, the scope of this study is to investigate the effects of blocking on seasonal surface temperature anomalies for the annual climate of Turkey. This study is unique due to three aspects regarding the climate of Turkey that will be investigated here. This is the first climatological study about blocking that focuses exclusively on Turkey. There are some studies that focus on blocking activity and climate in the Eurasian region but they mention Turkey only briefly (e.g., Sousa *et al*., 2016; 2017). Secondly, a large observational data set of surface temperature is used in this study to identify the temperature characteristics for several stations in Turkey during blocked days and compares these to non-blocked days. Lastly, this is the first study that investigates the effects of blocking on temperature anomalies during all seasons for our study region using a more varied set of blocking characteristics including BI.

2 | DATA AND METHODOLOGY

2.1 | Blocking data

The 500 hPa geopotential height data are provided by the National Centers for Environmental Prediction (NCEP) and National Center for Atmospheric Research (NCAR) Re-analysis-1 dataset (Kalnay *et al*., 1996), and these were used to detect atmospheric blocking events. The data are available from 1948 to present with 6-hr temporal resolution and $2.5° × 2.5°$ spatial (lat–lon) resolution. There are numerous data types available for both the surface and pressure levels. The NCEP–NCAR Re-analysis 500 hPa data set is used in several studies to detect blocking (e.g., de Vries *et al*., 2013; Mokhov *et al*., 2014; Sitnov *et al*., 2014). The daily geopotential data (0000 UTC) were used in this study for the period January 1, 1977–December 31, 2016. The zonal and meridional boundaries of the study region are 20°W–90°E and 30°N–90°N, respectively. The domain is shown as a background map (Figure 3) in the analysis section.

2.2 | Temperature data

Turkey is located on both the European and Asian continents and has complex topography. The largest portion of the country is in Southwest Asia. The northern portion is in extreme Southeast Europe. The Turkish State Meteorological Services provided the data for daily mean temperature at 77 stations distributed across the country during the aforementioned period. The location and altitudes of each station is presented in Figure 1. In order to enhance the readability of Figure 1, the first three letters of the stations' names are used to represent the stations.

2.3 | Detection of blocking and blocking index

The blocking detection method used in this study was described in TM90, which is based on the original objective
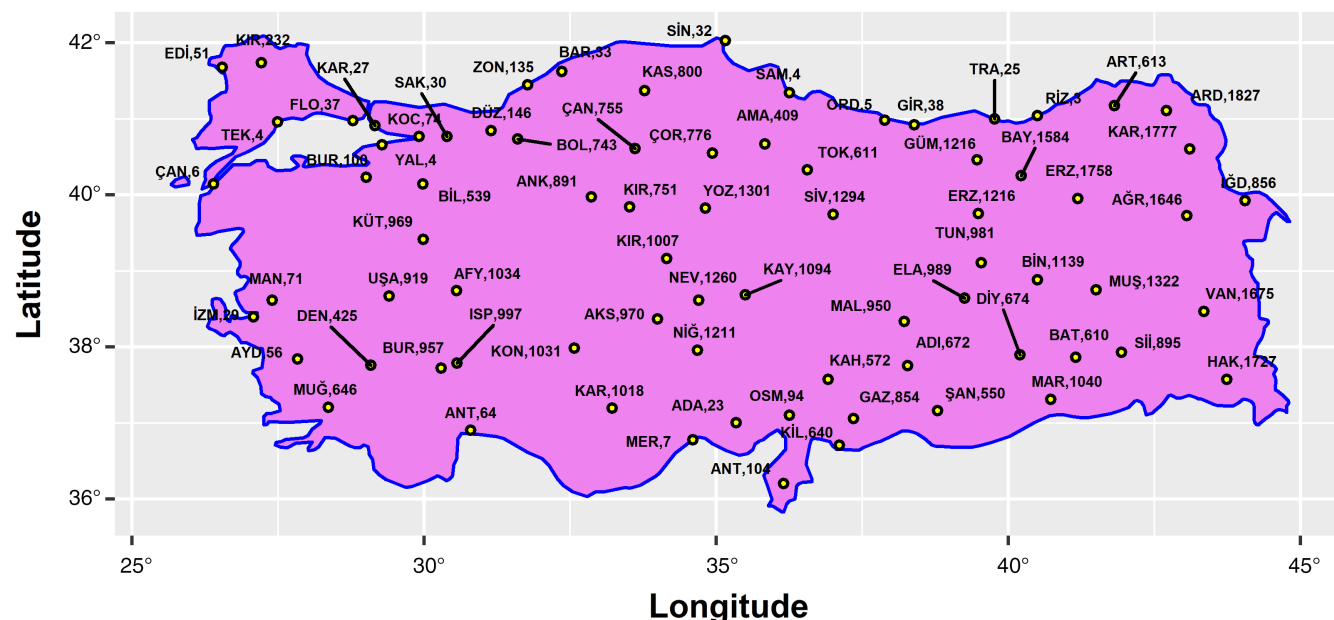
FIGURE 1 The weather stations of Turkish State Meteorological Service used here [Colour figure can be viewed at wileyonlinelibrary.com]

criterion published by Lejenäs and Økland (1983). For the TM90 method, two 500-hPa geopotential gradients are computed for each longitude and every day as in Equation (1);

$$GHGS = \frac{Z_{\lambda,\varphi_0} - Z_{\lambda,\varphi_S}}{\varphi_0 - \varphi_S}$$

$$GHGN = \frac{Z_{\lambda,\varphi_N} - Z_{\lambda,\varphi_0}}{\varphi_N - \varphi_0} \qquad (1)$$

$$\varphi_S = 40^{\circ} + \Delta, \varphi_0 = 60^{\circ} + \Delta, \varphi_N = 77.5^{\circ} + \Delta \text{ and}$$
$$\Delta = -5^{\circ}, -2.5^{\circ}, 0, 2.5^{\circ}, 5^{\circ} \qquad (2)$$

where $Z_{\lambda,\varphi}$ is the geopotantial height at the longitude λ and latitude φ. The geopotential height gradient in southern part of φ_0 (GHGS) is proportional to the zonal component of the geostrophic wind and geopotential height gradient in northern part of φ_0 (GHGN) is included in order to exclude non-blocked flows. This modified version of TM90 is based on the availability of the NCEP–NCAR data with $2.5^{\circ} \times 2.5^{\circ}$ resolution. An arbitrary longitude is accepted as blocked when both GHGS and GHGN verify the condition expressed by Equation (3) for at least one of the five Δ values and simultaneously the geopotential height gradient at φ_0 is positive. By allowing five Δ values, this criterion provides for more blocking opportunities and better spatial resolution instead of three Δ proposed by TM90;

$$GHGS > 0$$

$$GHGN < -10 \, gpm/^{\circ}lat$$

$$Z(\lambda, \varphi_0) - \overline{Z(\lambda, \varphi_0)} > 0 \qquad (3)$$

A region can be assumed as blocked when a considerable number of adjacent longitudes are simultaneously blocked since blocking events are large-scale phenomena. In this study, consistent with (Barriopedro et al., 2006) five or more adjacent grid points (12.5°) are required to confirm that a blocking event exists, with the allowance of one non-blocked longitude between the blocked longitudes.

There is no temporal persistence criterion accepted by all blocking studies, even though duration is one of the most important characteristics of blocking event. Most authors use 5 days as the minimum duration criteria (Treidl et al., 1981; Lupo and Smith, 1995; Shabbar et al., 2001; Scherrer et al., 2006), and this definition is adopted for our study as well.

The blocking centre is defined as "the compound of latitude that has the greatest longitudinal average of geopotential height and longitude that has the greatest latitudinal average of geopotential height" by using the method that was described in (Barriopedro et al., 2006). BI was calculated as "the ratio of geopotential height at the blocking centre to the geopotential height at the box boundaries" according to the method described by Wiedenmann et al. (2002). The temporal algorithm was executed for tracking blocking events (except step two) as was described in (Barriopedro et al., 2006). According to this algorithm, the blocking event must last at least 5 days. However, a non-blocked day between two blocked days is considered as blocked and it is considered as the same blocking event if the area blocked at day i intersects the area blocked at day $i + 1$.

2.4 | Statistical relationships

The Pearson correlation coefficient (Pearson, 1896) is used to determine the relationship between blocking properties and temperature anomalies. The significance of the relationship was tested by using the t-distribution with $N - 2$ degrees of freedom. The anomalies during blocked days were stratified by season (December, January and February for winter; March, April and May for spring; June, July and August for summer and September, October and November for fall). The seasonal temperature anomalies for all stations are categorized into five classes: Very Strong Negative (anomaly $< \mu - 2\sigma$), Strong Negative ($\mu - 2\sigma <$ anomaly $< \mu - \sigma$), Near-normal ($\mu - \sigma <$ anomaly $< \mu + \sigma$), Strong Positive ($\mu + \sigma <$ anomaly $< \mu + 2\sigma$) and Very Strong Positive ($\mu + 2\sigma <$ anomaly) where μ and σ represents the seasonal mean and standard deviation of the temperature anomaly, respectively. In this categorization, we use positive and negative to demonstrate the strength of the anomaly with reference to the mean, not the absolute magnitude of the anomaly. All figures except advection maps are illustrated via ggplot2 R-package (Wickham, 2016). All calculations are done via R-programming (Wickham et al., 2017; R Core Team, 2018).

3 | RESULTS

3.1 | Blocking

The statistical characteristics of atmospheric blocking events with respect to seasons in the study domain are calculated and shown in Table 1. The maximum value for mean block duration occurs during the winter and spring seasons at 9.2 days. The fall season has the minimum block duration at 8.1 days, while the value for the mean annual duration is 8.8 days. The mean occurrence for atmospheric blocking events is nearly the same during winter, summer and fall at

TABLE 1 The characteristics of the blocking events in the domain

	Winter	Spring	Summer	Fall	Annual
Mean duration (days)	9.24	9.21	8.4	8.1	8.8
Count	2.7	3.9	2.5	2.6	11.7
Intensity	2.65	2.31	1.91	2.4	2.41
Longitudinal extent (degrees)	29	27	25	25	28

2.7, 2.5 and 2.6 events, respectively. In contrast, spring has more blocking occurrences than any other season (3.9 events). This is consistent with Lupo *et al*. (2019) for the Atlantic Region and Northern Hemisphere in recent years. The mean annual value for atmospheric blocking occurrences within the study region is 11.7.

The mean seasonal values for BI range between 1.91 and 2.65 in the study area. The most intense blocking events are observed in winter (2.65), while the weakest blocking events are observed in summer (1.91). Spring and fall have nearly the same values for BI, 2.31 and 2.36, respectively. These results including the seasonal variability are consistent with Wiedenmann *et al*. (2002) or Barriopedro *et al*. (2006) for their Atlantic region climatologies. The annual mean BI is 2.41 in the study domain.

The last blocking characteristic examined here is the longitudinal extent as measured by degrees longitude. The seasonal longitudinal extent fluctuates between 25° and 29° longitude. The longitudinal extent of atmospheric blocking is the largest in winter (29° longitude), while spring (27° longitude) had the second largest extent and summer and fall had a nearly the same longitudinal extent (25° longitude). The annual mean extent for atmospheric blocking is 28° longitude.

Block size and duration were positively correlated here (r = 0.3, 0.3, 0.18 [*not statistically significant*, *hereafter*, *NSS*], 0.40 for winter, spring, summer and fall, respectively) as well as block size and BI (r = 0.5, 0.56, 0.54, 0.65 for winter, spring, summer and fall, respectively) and these were statistically significant at the 95% confidence level. The exception was for block size and duration in summer, and all these results are consistent with Lupo and Smith (1995), especially for the winter season. Lupo and Smith (1995) showed these relationships were strongest in the Atlantic sector as well.

3.2 | General pattern of temperature anomalies

The mean seasonal temperature anomalies during blocked and non-blocked days are examined. Additionally, the composite map of 500 hPa geopotential height for the 10 events associated with the coldest and warmest conditions as well as representative temperature advection maps for these

events are also investigated to explain the dynamics contributing to these temperature anomalies.

3.2.1 | Temperature anomaly during blocked days

The seasonal mean temperature anomalies during blocked days varied between −2.1 and 0.8°C (Figure 2). The Kırklareli station and Trakaya sub-region stations in the Marmara Region of Turkey had the highest negative temperature anomalies in winter with −2.1 and −2.0°C, respectively, although the Ağrı station in the East Anatolia Region has the highest positive temperature anomaly during spring with 0.8°C.

As seen in Figure 2 there are mainly four temporal patterns for the mean seasonal temperature anomalies. The first pattern (P1b) can be characterized with the minimum temperature anomaly in winter, increasing towards 0°C or above during spring, then slightly increasing or decreasing during the summer and finally a sharp decrease towards negative values in fall. For P1b, the highest negative temperature anomaly was observed during the winter. This pattern is usually observed for cities that are on the shore of Black Sea, Marmara Sea and the northern part of the Aegean Sea. The same pattern is observed for the Kutahya, Tokat, Nevşehir, Kayseri and Yozgat stations even though they are located within the inner part of Turkey.

The second pattern (P2b) is characterized by the cold seasons (winter and fall) observing negative temperature anomalies with nearly the same magnitude. During the warm seasons (spring and summer), the temperature anomalies were close to 0°C. This pattern is observed within Central Anatolia and the inner part of Aegean Region and Black Sea Region. For a majority of the cities that observe P2b, the temperature anomaly during the summer season was about 0.2°C lower than that for the spring season. For the other stations with P2b, the warm season temperature anomalies are of similar magnitude.

The third pattern (P3b) can be described as negative temperature anomalies in winter, then anomalies increasing to +0.5°C in spring, and finally decreasing towards negative values for both summer and fall. The P3b is observed within the Eastern and Southeast Anatolia Regions. This pattern, however, can be split into two sub-categories. The first sub-category is associated primarily with northern cities and has
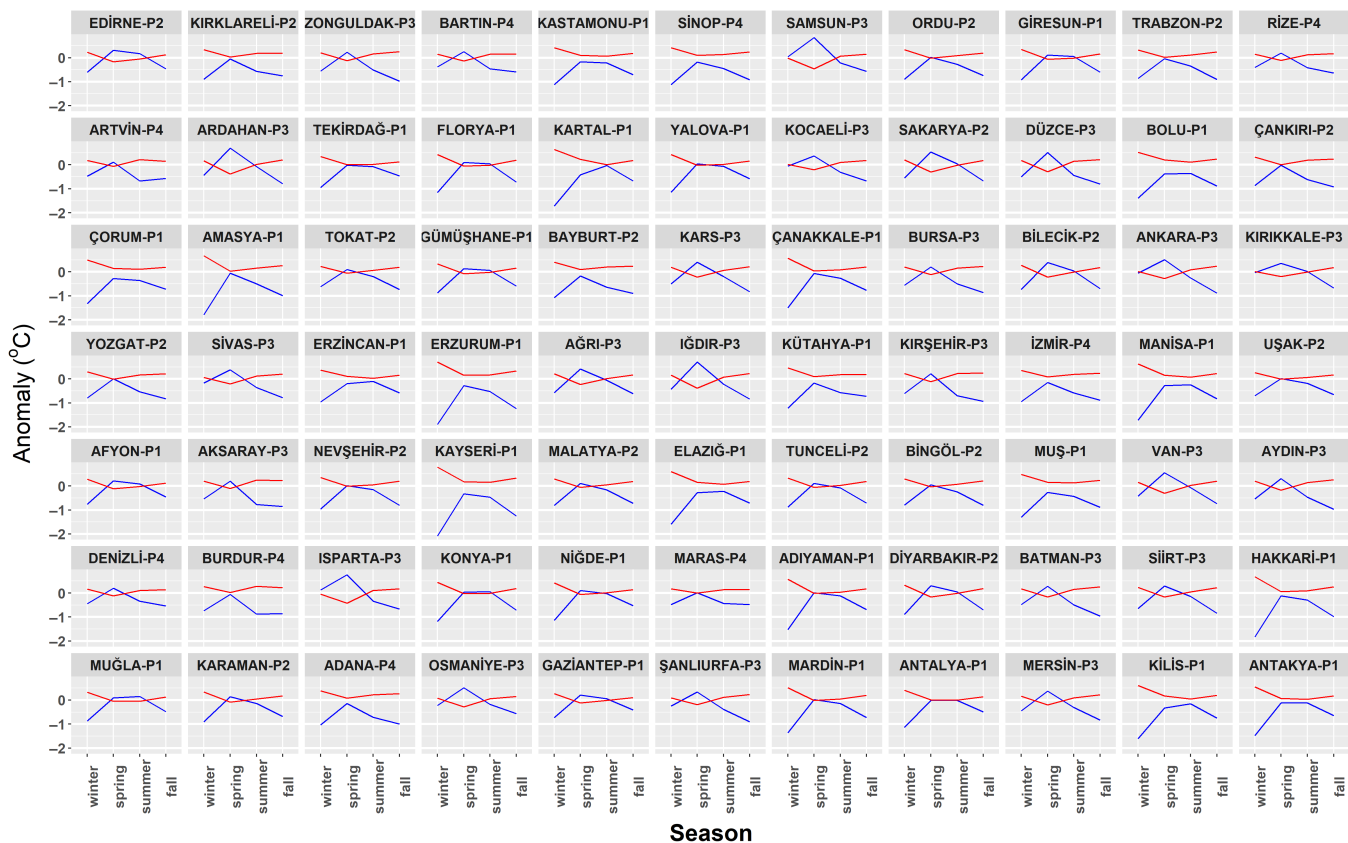
FIGURE 2 Mean seasonal temperature anomaly (°C) during blocked days (blue line) and non-blocked days (black line) [Colour figure can be viewed at wileyonlinelibrary.com]

lower temperature anomalies during winter than in summer. For the other sub-category, the pattern has nearly identical anomalies for both winter and summer or even lower summer season temperature anomalies. This pattern is observed primarily within the southernmost part of Southeast Anatolia Region.

The fourth pattern (P4b) is observed within the cities of the Mediterranean Sea Region and south of the Aegean Sea. For P4b, the spring season was associated with the maximum temperature anomalies near 0°C and the other seasons observe close to the same negative anomalies.

The mean 500 hPa geopotential height fields during the blocking events associated with the 10 coldest and the 10 warmest surface temperature anomalies were stratified by season (Figure 3). Turkey is on the downstream flank of the blocking high (Figure 3a,c,e,g) and exposed to cold air advection (Figure 4a,c,e,g) during the coldest events. This is a similar configuration for eastern Pacific blocking events in relation to cold conditions in the central United States (e.g., Nunes *et al.*, 2017). On the other hand, Turkey is exposed to warm air advection (Figure 4b,d,f,h) during blocking events that are located downstream of the study region (Figure 3b,d,f,h). As seen in Figure 4, the magnitude of the advection fields upstream of blocking events are

greater than the magnitude of the advection fields downstream of blocking events for each season.

3.2.2 | Temperature anomaly during non-blocked days

Temperature anomalies during non-blocked days varied between −0.5°C (Ağrı in spring) and 0.75°C (Edirne in fall). Similarly, the temperature anomaly annual cycle during non-blocked days can be categorized into four groups with different behaviour (Figure 2).

The first pattern (P1n) can be described as follows; the highest positive temperature anomalies were observed during winter season, then decreasing values for temperature anomalies in warm seasons and increasing values in the fall. This pattern is observed within the cities of the coastal region of Black Sea, Marmara Sea and northern Aegean Sea region. The mean seasonal anomalies are all positive in this pattern except at Rize and Ordu. These regions have nearly the same type of pattern as that for P1b blocked days, but of opposite sign.

The second pattern (P2n) is characterized by positive temperature anomalies of the same magnitude in cold seasons and anomalies around 0°C in warm seasons, but of
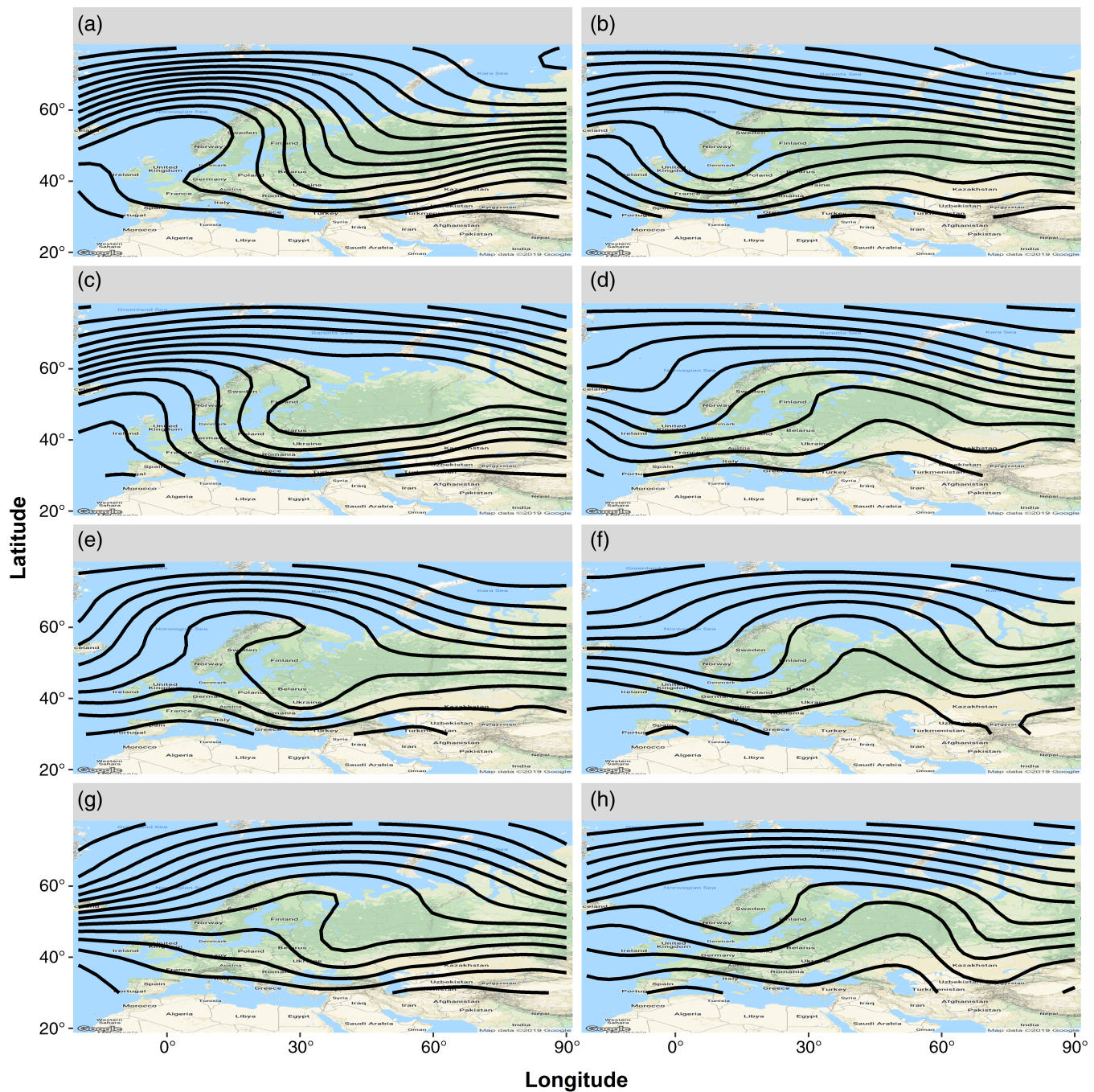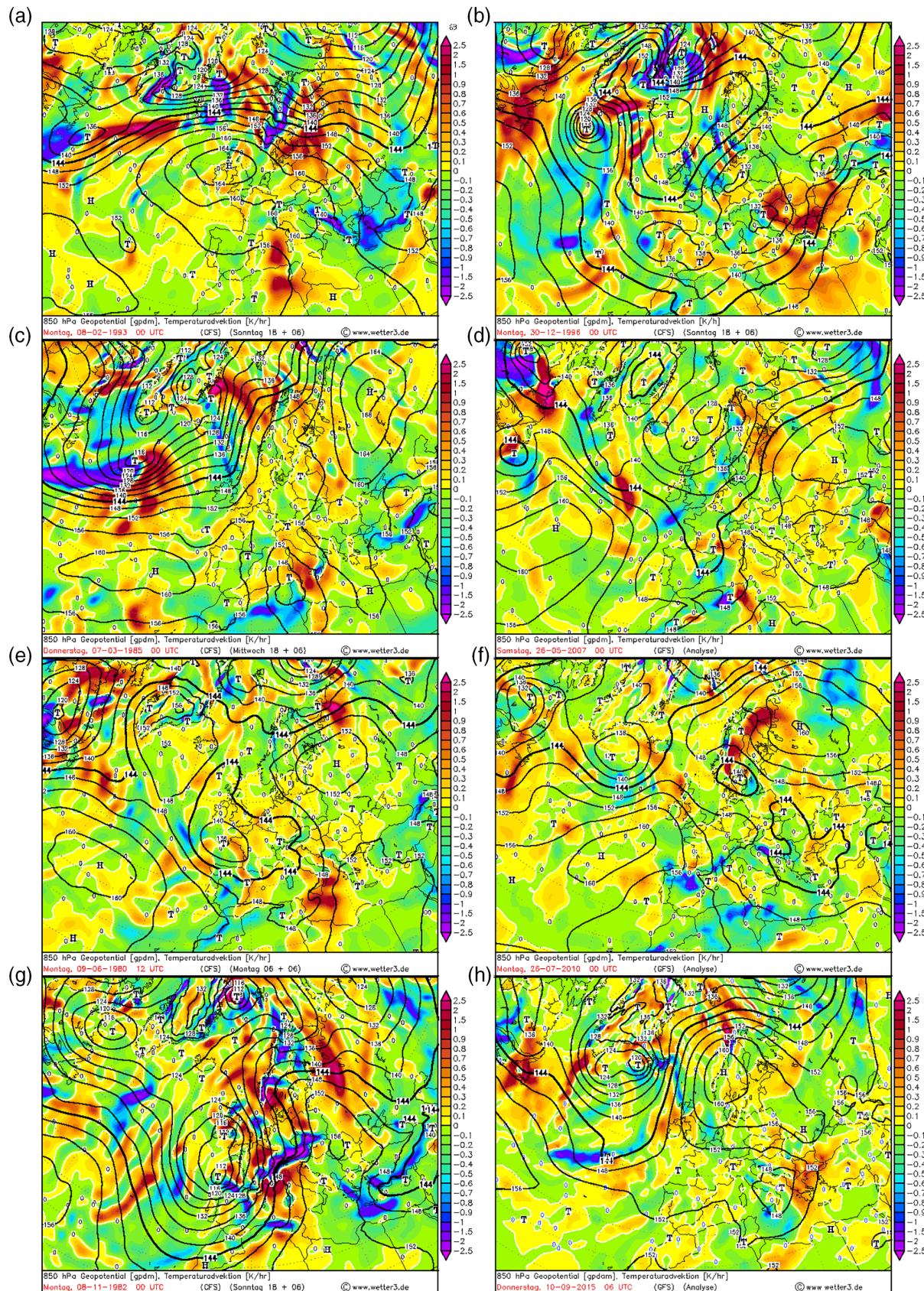
FIGURE 3 The average 500 hPa height (m) during (a) 10 coldest winter, (b) 10 warmest winter, (c) 10 coldest spring, (d) 10 warmest spring, (e) 10 coldest summer, (f) 10 warmest summer, (g) 10 coldest fall and (h) 10 warmest fall events [Colour figure can be viewed at wileyonlinelibrary.com]

opposite sign as P2b. Analogous to P2b, P2n is observed within the Central Anatolia Region and inner parts of Aegean Region and Black Sea Region. The northern cities have lower anomalies during the spring compared to summer (0.2°C lower). However, the southern cities have nearly equal anomalies around 0°C.

The third pattern (P3n) is observed within Eastern and Southeastern Anatolia. This pattern is associated with a positive temperature anomaly in winter, a negative minimum during spring and then a linear increase for the summer and fall seasons. The fall season has the greatest positive temperature anomaly for most of these stations. Only Erzincan and Sivas have greater temperature anomalies during winter than in fall.

The fourth pattern (P4n) is observed along the shore of Mediterranean Sea and the southern part of the Aegean Sea.

FIGURE 4 The representative 850 hPa temperature advection (K/s) for (a) 10 coldest winter, (b) 10 warmest winter, (c) 10 coldest spring, (d) 10 warmest spring, (e) 10 coldest summer, (f) 10 warmest summer, (g) 10 coldest fall and (h) 10 warmest fall events [Colour figure can be viewed at wileyonlinelibrary.com]

For P4n, the temperature anomalies within all seasons vary close to 0°C. Spring is associated with a negative anomaly, and the other seasons have positive anomalies of almost the same magnitude.

Lastly, the anomaly difference between blocked and non-blocked days' curve (not shown) would mirror the blocked days' curve in Figure 2 for almost all instances. This indicates the impact of blocking on observed surface temperature as blocked days comprised 30% of the study period.

3.3 | Relationship between blocking parameters and temperature anomaly

The relationship between the following blocking parameters; BI, duration, longitudinal extent and surface temperature anomalies are investigated and stratified by season. Here the Pearson correlation coefficients are calculated and tested using the t test in order to establish a statistical relationship. The results that are statistically significant at 95% confidence level will be the main focus of this discussion. Additionally, we chose 28 representative stations and investigated the relationship between blocking parameters and temperature anomalies in order to test for pseudo-replication. However, this test did not alter significantly the conclusions below. It is acknowledged here also that there is a lot of spread in Figures 5–7 due to case-to-case variability of blocking events, including where these events occurred.

3.3.1 | Blocking intensity versus temperature anomaly

The relationship between BI and surface temperature anomaly is shown in Figure 5. The fall has a value of −0.31 (Figure 5d), while the winter (Figure 5a) and summer (Figure 5c) seasons have values of −0.27. As inferred from the correlation coefficient values, there is an inverse relationship between these for each season. In other words, stronger blocking events are associated with cooler surface temperatures.

3.3.2 | Blocking duration versus temperature anomaly

The winter season has a negative correlation coefficient with the value of −0.31, which is statistically significant at the 95% confidence level (Figure 6a). This result indicates an inverse relationship between mean block duration and mean surface temperature anomaly during blocking events. For this season, more persistent blocking events are associated with colder temperatures (Figures 3a and 4a). Combining the duration and BI, colder surface temperature anomalies are associated with both stronger more persistent blocks

located upstream of Turkey. Wiedenmann *et al.* (2002) found a significant correlation between block duration and BI especially during winter. Thus, the result here is consistent with Wiedenmann *et al.* (2002).

### 3.3.3 | Longitudinal extent of blocking versus temperature anomaly

The correlation coefficient between the mean longitudinal extent of blocking and mean temperature anomaly stratified by season varies between −0.24 and −0.1 and all of them are statistically significant at 95% confidence level (Figure 7). The winter and spring seasons were associated with values of −0.24 (Figure 7a) and −0.23 (Figure 7b), respectively. This indicates that a larger blocking event is associated with a colder surface temperature anomaly. Also, as suggested by Figure 7a,b, larger and stronger blocks are associated with colder anomalies. Lupo and Smith (1995) found a statistical relationship between larger blocks and stronger blocks, especially in the Atlantic region. The summer and fall seasons were associated with correlation values of −0.1 (Figure 7c) and −0.14 (Figure 7d).

## 3.4 | Temperature anomaly distribution during blocked days stratified by seasons

3.4.1 | Winter

The average temperature anomaly for stations in certain regions of Turkey during blocked days is stratified by season. The mean temperature anomalies during the winter season are shown in Figure 8a. The spatial mean anomaly is −0.86°C during the winter season with a standard deviation of 0.48°C. As seen in Figure 8a, the entire country observes negative anomalies except four cities in the eastern part of the country. Very strong negative temperature anomalies are observed in the northwestern part of Turkey and strong negative anomalies are observed in Marmara region and some cities of Black Sea Region due to the strength of cold temperature advection associated with upstream blocking events and the relative weakness of warm temperature advection in the downstream blocking events (see Figures 3a,b and 4a,b).

In the southeast part of the country, strong positive anomalies are observed across most of Turkey and a very strong positive anomaly was observed in only Muş. This situation is due to relatively weak cold air advection in upstream blocking events and strong warm air advection in downstream blocking events (Figures 3a,b and 4a,b). Near-normal temperature anomalies were observed in the Central Anatolia Region, Mediterranean Region, Aegean Region and several cities from Black Sea Region due to weak values for temperature advection associated with both upstream and downstream blocking events.
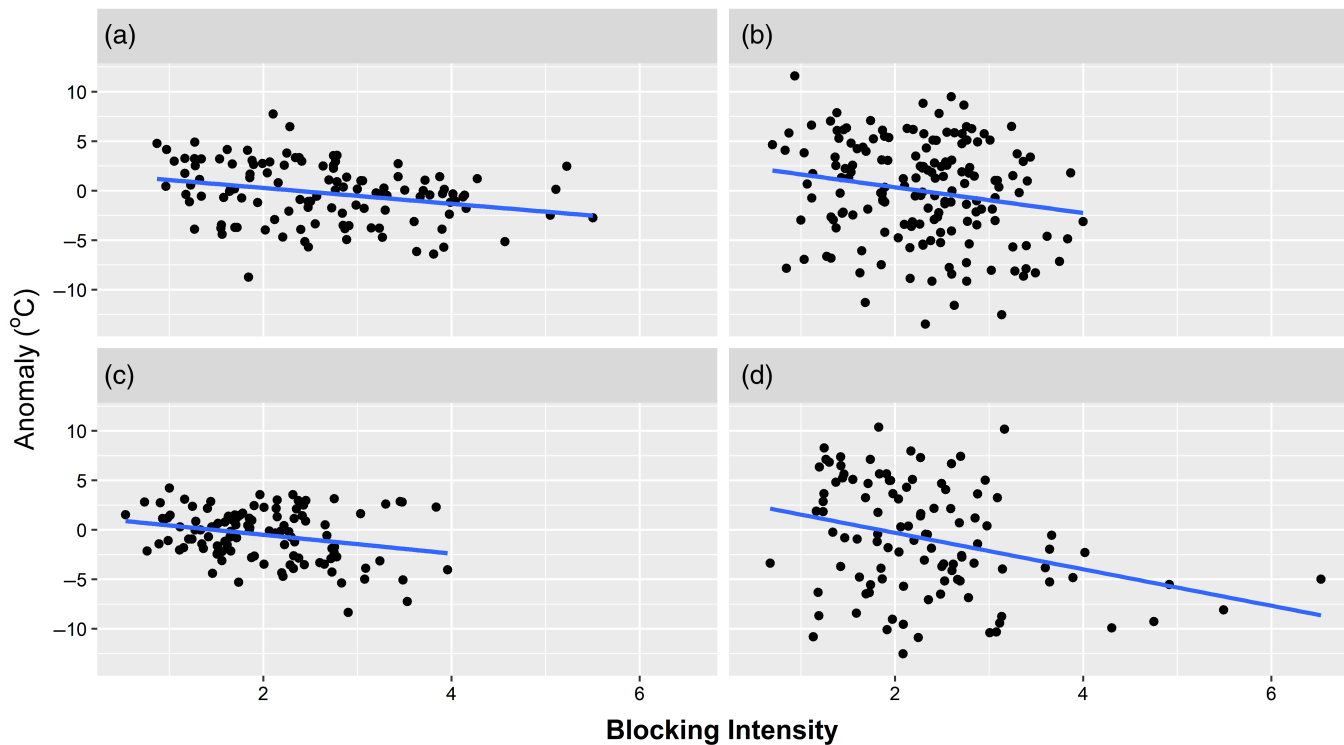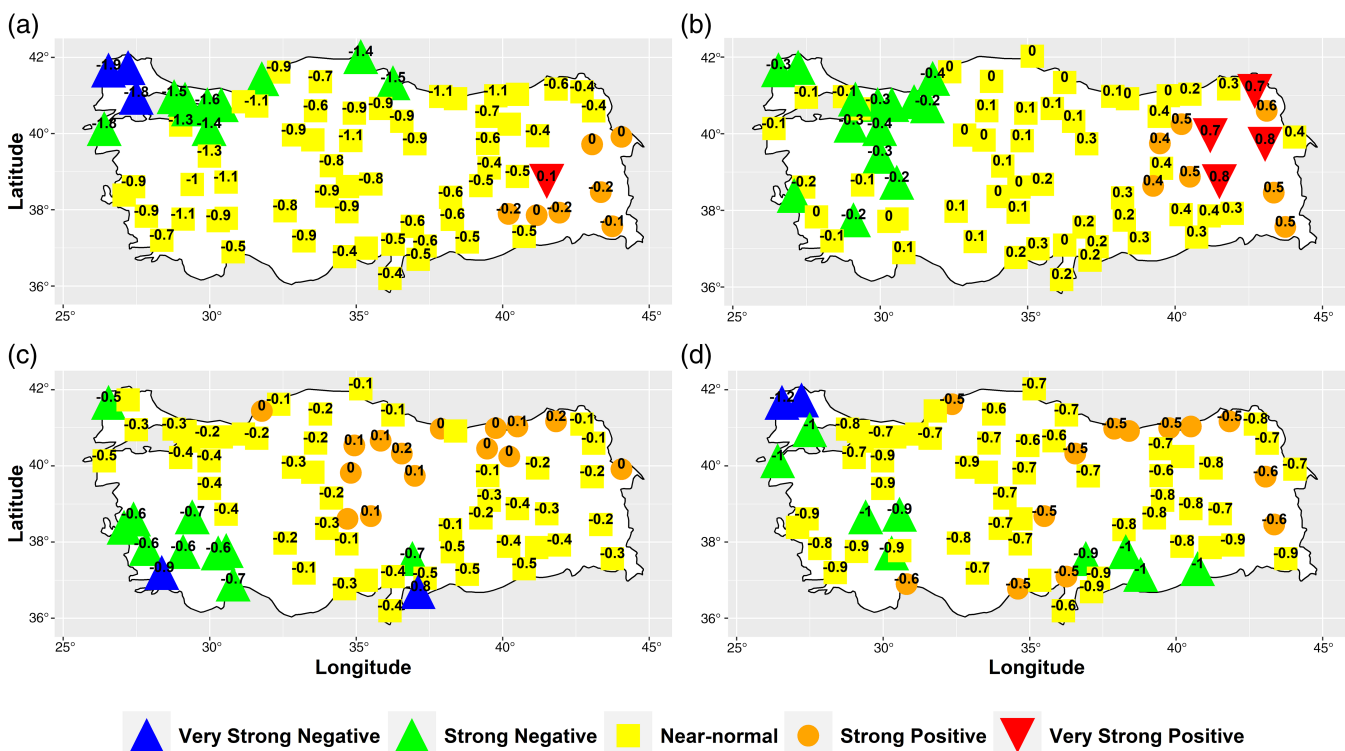
FIGURE 5 Relationship between BI and mean temperature anomaly (°C) during (a) winter, (b) spring, (c) summer and (d) fall. BI, block intensity [Colour figure can be viewed at wileyonlinelibrary.com]
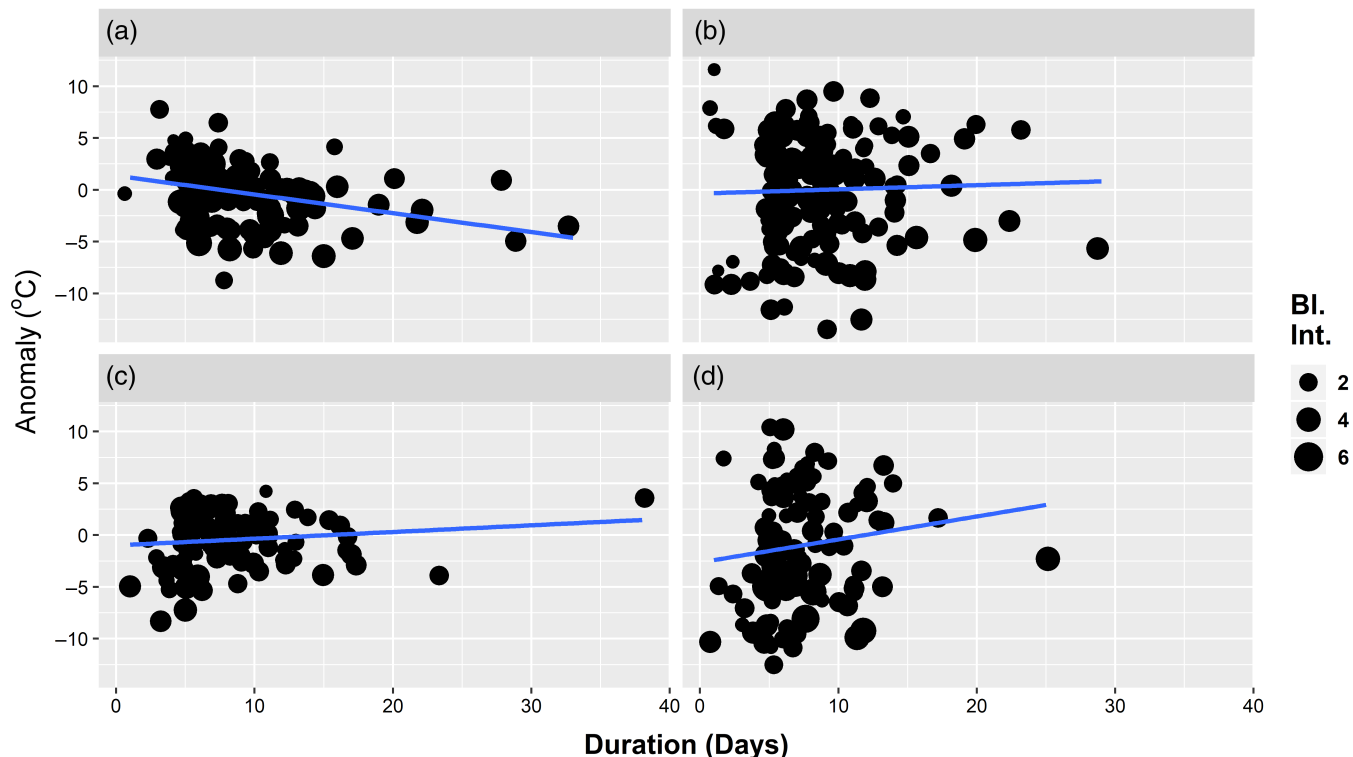
FIGURE 6 Relation between blocking duration (days) and mean temperature anomaly (°C) during (a) winter, (b) spring, (c) summer and (d) fall. The colour of the points indicates the different BI values. BI, block intensity [Colour figure can be viewed at wileyonlinelibrary.com]
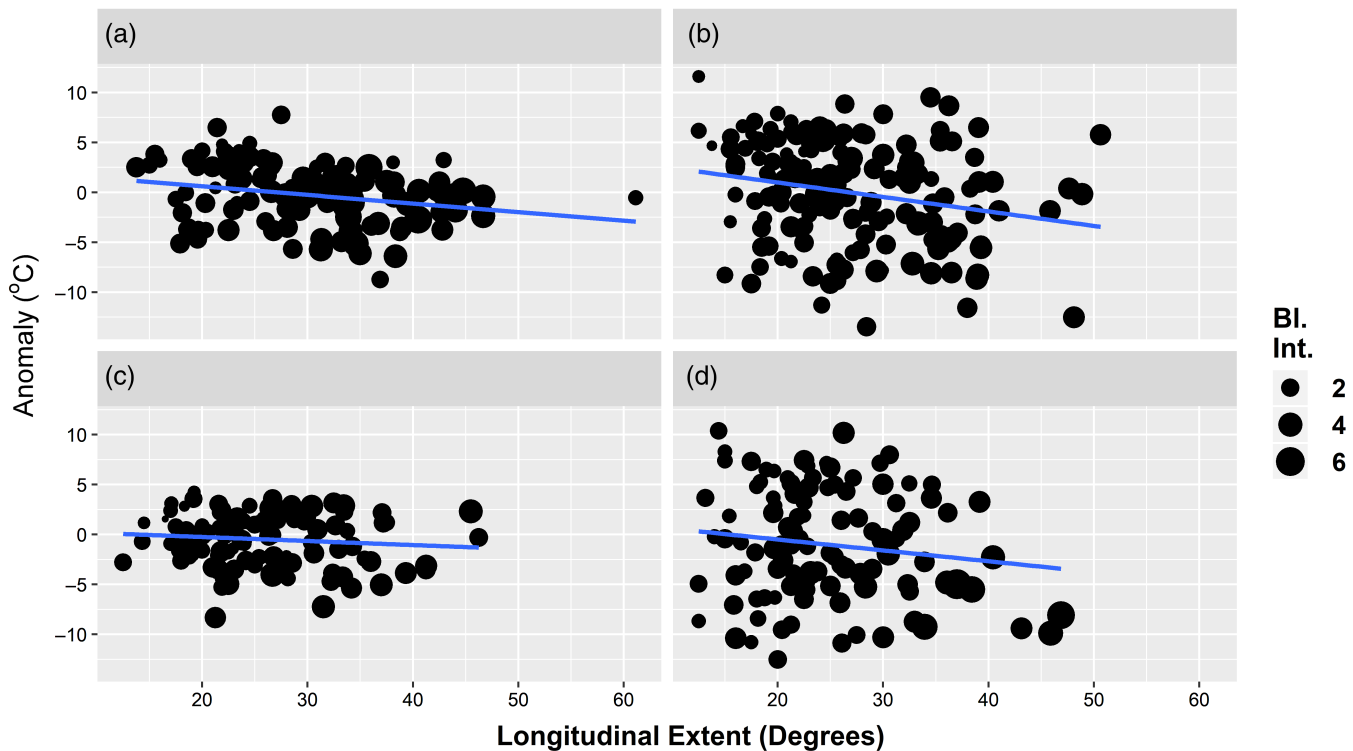
FIGURE 7   Relation between blocking longitudinal extent in number of longitudes and mean temperature anomaly (°C) during (a) winter, (b) spring, (c) summer and (d) fall. The colour of the points indicates the different BI values. BI, block intensity [Colour figure can be viewed at wileyonlinelibrary.com]

FIGURE 8   Mean temperature anomalies (°C) in stations in (a) winter, (b) spring, (c) summer and (d) fall during blocked days [Colour figure can be viewed at wileyonlinelibrary.com]

3.4.2 | Spring

The mean temperature anomalies during the spring season are shown in Figure 8b. The spatial average of seasonal temperature anomaly is 0.11°C with a standard deviation of 0.28°C. During this season, it is shown that the western portion of the country has strong negative and near-normal anomalies, the central region has near-normal anomalies and the eastern part has near-normal, strong positive, to very strong positive anomalies. Similarly, the western area is strongly affected by cold air advection, the eastern region is strongly influenced by warm air advection (Figures 3c,d and 4c,d). Very strong negative anomalies were not observed during this season (Figure 8b) likely because the cold air advection during this season is not as strong as cold air advection during the winter (Figures 3a–d and 4a–d).

Strong negative anomalies were observed over the continental region of Northwest Anatolia, the eastern region of the Marmara Region, the western part of Black Sea Region and several of the stations in the Aegean Region. The remaining stations in the Marmara and Aegean Region have near-normal anomalies. Almost the entire central Anatolia Region, Black Sea coastline except the western part, the Mediterranean coastline and the Southern Anatolian Region have near-normal temperature anomalies. Bayburt, Erzincan, Elazığ, Bingöl, Kars, Van and Hakkari stations from East Anatolian Region has strong positive temperature anomalies. Lastly, Ardahan, Ağrı, Erzurum and Muş have very strong positive anomalies.

3.4.3 | Summer

The spatial average of temperature anomalies within Turkey during the summer season is −0.27°C and the standard deviation is 0.24°C (Figure 8c). The summer season temperature anomalies in Turkey did not show any distinct pattern. Only the Muğla station from the Aegean Region and Kilis from the Southeast Anatolia Region have very strong negative anomalies likely due to the location of both stations on the downstream flank of the blocking ridge during cold air advection (Figures 3e,f and 4e,f). In the southwest part of country, Edirne from the Marmara Region, and Kahramanmaraş from the Mediterranean Region have strong negative temperature anomalies during this season (Figure 8c). Similarly, these stations are located on the downstream flank of a ridge during cold air advection situations (Figures 3e,f and 4e,f).

The eastern cities of the Central Anatolia Region, several cities of the east of Black Sea Region, including Zonguldak from west Black Sea Region, and Iğdır from East Anatolia Region have strong positive temperature anomalies (Figure 8c). These regions are not typically exposed to cold temperature advection during upstream blocking events, but are impacted by warm temperature advection during downstream blocking events (Figures 3e,f and 4e,f). The rest of the country has near-normal temperature anomalies, and very strong positive anomalies are not observed at any station.

3.4.4 | Fall

The fall season temperature anomalies are negative throughout nearly the entire country. The spatial average of the anomaly is −0.75°C, with 0.16°C standard deviation. The distribution of temperature anomalies during the fall is complex (Figure 8d), and there is not a prominent or coherent pattern. The Edirne and Kırklareli stations have very strong negative temperature anomalies. The southwest part of the Marmara Region, the Southeast Aegean Region and east of the South East Region have strong negative temperature anomalies. These regions are located on the downstream flank of the ridge during cold blocking events and not typically affected by the warm temperature advection during downstream blocking events (Figures 3g,h and 4g,h).

The Antalya, Mersin and Osmaniye stations from the Mediterranean Region, Kayseri from the Central Anatolia Region, Bartın from west of the Black Sea Region, east of the Black Sea Region and Ağrı and Van from the East Anatolia Region have strong positive temperature anomalies. These regions are located within a flow regime in which the height contours are zonally aligned during cold events and more often affected by warm air advection during upstream blocking events (Figures 3g,h and 4g,h). The rest of the country has near-normal anomalies, while none of the stations observed very strong positive anomalies.

3.5 | 500 hPa conditions during extreme temperature anomalies

In this section, the average 500-hPa geopotential height conditions for two case studies representing the maximum and minimum temperature anomalies were examined.

3.5.1 | Maximum warm anomaly

The average temperature anomaly across Turkey during September 8–13, 2015 is 10.4°C. The average geopotential heights at the 500 hPa level during this period are shown in Figure 9a. There was a dipole blocking (Rex-type blocking) event centred at ~65°N and 10°E. The accompanying low centre is located at about 53°N and 15°E. Turkey is located under the southeastern part of the low-pressure centre. Thus, there is warm air temperature advection as a result of the transport of air from the Mediterranean and Sahara region west of Turkey. This blocking event dominated the weather
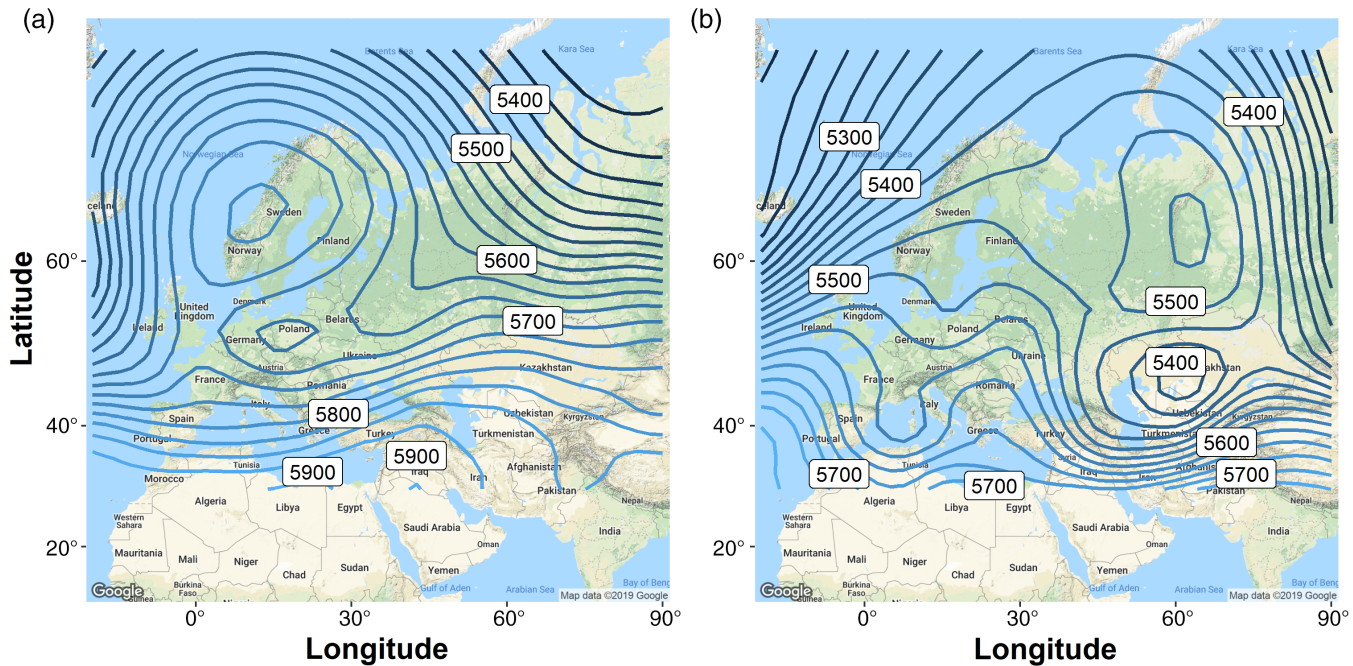
FIGURE 9   The average 500 hPa geopotential height (m) for the period of (a) September 8–13, 2015 (the blocking event with greatest temperature anomaly), and (b) March 3–11, 1985 (the blocking event with lowest temperature anomaly) [Colour figure can be viewed at wileyonlinelibrary.com]

of early September 2015 over Europe as well, and the BI for this event was 3.56; a value typical for the fall season over the Atlantic Region (see University of Missouri Blocking Archive: http://weather.missouri.edu/gcc). The result was generally cooler than normal conditions for Northwest Europe and warmer than normal conditions over central and Eastern Europe, including Turkey (Weather Log, 2015).

It is possible that the warm advection influencing Turkey is not directly attributable to blocking, but is an indirect impact. Many studies (e.g., Hong *et al*., 2011; Lau and Kim, 2012; Lupo *et al*., 2012; Luo *et al*., 2015; Nunes *et al*., 2017) have demonstrated that blocking results in persistent temperature or precipitation anomalies in the up or downstream directions. In order to compare the impact of a similarly located transient ridge event on Turkey with the blocking event, a typical transient event was identified (Figure 10).The ridge over Scandinavia during December 31, 2017 and corresponding 850 hPa temperature advection is plotted. As seen in Figure 10, this ridging event over Scandinavia is associated with cold air advection over western part of the Turkey (Figure 10b).

3.5.2 | Maximum cold anomaly

The average 500-hPa geopotential heights during the period March 3–11, 1985 are shown in Figure 9. During this period, the average temperature anomaly for Turkey was −13.7°C. As seen in Figure 9b, the blocking event was

located northeast of Turkey. In this case, the block centre was located at ~60°N and 60°E. Similarly, this event is also a Rex-type blocking event. The low centre is located at about 45°N and 60°E. During this period, cold air originating from the North Atlantic and possibly also from Russia was transported into Turkey. This blocking event was tilted positively (from southwest to northeast) and thus, colder air was drawn from the polar regions directly towards the study region implying less modification of the surface air mass. This is consistent with Luo *et al*. (2015) and Yao *et al*. (2016), who demonstrated that the tilt of the blocking axis was important for impacting regional weather. The BI (2.32) for this blocking event was also typical of the region and season, and persisted for much of the early part of March 1985 (University of Missouri Blocking Archive). This event contributed to cooler than normal temperatures for this month, as noted by Radcliffe (1985).

4 | DISCUSSION AND CONCLUSION

Using the NCEP and NCAR re-analyses and data acquired from the Turkish State Meteorological Service, the difference between blocked and non-blocked temperature anomalies were compared for Turkey from 1977 to 2016. An analysis of the climatological characteristics for blocking events that impacted Turkey was also examined, and finally the relationship between blocking characteristics and temperature anomalies were also studied. The analysis included

(a)
(b)
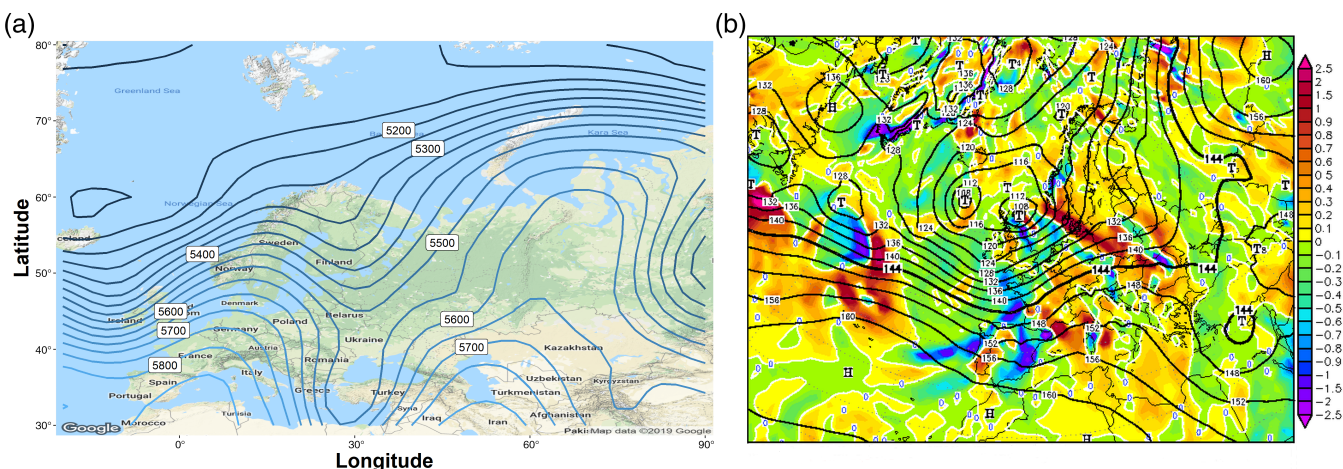
FIGURE 10 (a) 500 hPa geopotential height (m) and (b) 850 hPa temperature advection (K/s) for the transient ridging event on December 31, 2017 [Colour figure can be viewed at wileyonlinelibrary.com]

an examination of composite blocking events for each season as well as two case studies for blocking events associated with the most extreme temperature anomalies over Turkey. An investigation of the impact of blocking on not only temperature but also any meteorological parameter of Turkey has not been done previously. Thus, the following results are new and will provide an operational community with forecast guidance under blocking situations.

The main characteristics of blocking in the study region during study period can be explained briefly as follows. The mean duration of blocking events impacting Turkey is 8.8 days, with maximum of 9.2 days in both winter and spring and the minimum of 8.1 days in summer. The mean occurrence of blocking is 11.7 events per year with the maximum of 3.9 events in spring and 2.5 events in summer. The most intense blocking events are observed in winter (2.50) and weakest events are observed in summer (1.91). The mean longitudinal extent is 28° longitude with the maximum in winter (29° longitude) and minimum in summer (25° longitude).

Blocking events play a crucial role on the temporal distribution of the mean seasonal temperature anomaly of all stations even though BF is around 30% during the year. There were four main patterns are observed for temperature anomalies during blocked days and non-blocked days. The northwest part of Turkey experiences negative temperature anomalies during all seasons in association with blocking. This is compatible with the results of Sousa *et al.* (2017) who showed that Southeast Europe (includes the northwestern part of the Turkey) has a negative maximum temperature anomaly during winter regardless of the domain that blocking occurs.

The spatial distribution of temperature anomalies associated with blocking were examined as well. The northwest part of Turkey experiences strong or very strong negative

cold temperature anomalies during blocked days for all seasons. This region is located on the downstream flank of a ridge during blocking events and is the most affected by cold air advection. The west part of the country experiences very strong, strong or near-normal negative temperature anomalies; the central part experiences near-normal negative anomalies at most stations. The eastern part of the country has near-normal temperature anomalies which is consistent with the location of blocking. This situation is not inconsistent with Sillmann *et al.* (2011), and they noted that Baltic Sea coast line is a major region that is influenced by atmospheric blocking. However, their study focuses on only the North Atlantic Blocking during the winter months.

Additionally, blocking events that impact Turkey are largest, strongest and most persistent during the winter season and there is a statistical relationship between the strength of the cold anomalies and block size, duration and persistence as in Lupo and Smith (1995). During the other seasons these relationships were not as clear.

Lastly, the composite plot of 500 hPa geopotential height shows that both coldest (March 1985) and warmest temperature anomalies (September 2015) are associated with a Rex-type block. As seen here, the tilt of the blocking axis plays an important role as mentioned in Luo *et al.* (2015) and Yao *et al.* (2016). March 1985 was one of the most memorable winter periods in Turkey because of heavy snow that influenced all of the Istanbul Region as well as the greater northwestern part of the country. All schools and government institutions were closed because transportation was halted due to the extreme snow depth. Also, a second atmospheric blocking event associated with very cold temperature anomalies was observed during March 1987 (not shown). Again, during that period the schools and government institutions were closed. It was mentioned in a previous study that the cause of the 1987 cold wave was a blocking event

(see Tayanç *et al*., 1998). The warmest event has no memorable effects due to its short duration.

Additionally, Nunes *et al*. (2017) demonstrated that during ten extremely cold months for the Belgorod Region of Southwest Russia (1944–2015), atmospheric blocking was observed over Europe, while for extremely warm months, blocking was located over the region or east of the region. This is true for Turkey as well based on the case studies here. Finally, the results here could provide guidance to operational forecasters or policy makers when blocking is anticipated in short range or long-range forecasts.

ACKNOWLEDGEMENTS

CONFLICT OF INTEREST

The authors declare no conflict of interest.

ORCID

Bahtiyar Efe https://orcid.org/0000-0001-5604-7068
Anthony R. Lupo https://orcid.org/0000-0002-5810-5652

REFERENCES

Antokhina, O.Y., Antokhin, P.N., Martynova, Y.V. and Mordvinov, V. I. (2016) The impact of atmospheric blocking on spatial distributions of summertime precipitation over Eurasia. *IOP Conference Series: Earth and Environmental Sciences*, 48, 12035. https://doi.org/10.1088/1755-1315/48/1/012035.

Antokhina, O.Y., Antokhin, P.N., Devyatova, E.V. and Martynova, Y. V. (2018) Wintertime atmospheric blocking events over Western Siberia in the period 2004-2016 and their influence on the surface temperature anomalies. *The 2nd International Electronic Conference on Atmospheric Sciences (ECAS 2017), 16–31 July 2017: Sciforum Electronic Conference Series*, Vol. 2, pp. 1–9.

Barriopedro, D., García-Herrera, R., Lupo, A.R. and Hernández, E. (2006) A climatology of northern hemisphere blocking. *Journal of Climate*, 19(6), 1042–1063. https://doi.org/10.1175/JCLI3678.1.

Brunner, L., Hegerl, G.C. and Steiner, A.K. (2017) Connecting atmospheric blocking to European temperature extremes in spring. *Journal of Climate*, 30, 585–594. https://doi.org/10.1175/JCLI-D-16-0518.1.

Cheung, H.N., Zhou, W., Mok, H.Y., Wu, M.C. and Shao, Y. (2013) Revisiting the climatology of atmospheric blocking in the northern hemisphere. *Advances in Atmospheric Science*, 30, 397–410. https://doi.org/10.1007/s00376-012-2006-y.

Demirtaş, M. (2017) The large-scale environment of the European 2012 high-impact cold wave: prolonged upstream and downstream atmospheric blocking. *Weather*, 72, 297–301. https://doi.org/10.1002/wea.3020.

Diao, Y., Xie, S.P. and Luo, D. (2015) Asymmetry of winter European surface air temperature extremes and the North Atlantic Oscillation. *Journal of Climate*, 28, 517–530. https://doi.org/10.1175/JCLI-D-13-00642.1.

Dunn-Sigouin, E., Son, S.W. and Lin, D. (2013) Evaluation of northern hemisphere blocking climatology in the global environment multiscale model. *Monthly Weather Review*, 141(2), 707–727. https://doi.org/10.1175/MWR-D-12-00134.1.

Hong, C.-C., Hsu, H.-H., Lin, N.-H. and Chiu, H. (2011) Roles of European blocking and tropical-extratropical interaction in the 2010 Pakistan flooding. *Geophysical Research Letters*, 38, L13806. https://doi.org/10.1029/2011GL047583.

Jensen, A.D., Lupo, A.R., Mokhov, I.I., Akperov, M.G. and Reynolds, D.D. (2017) Integrated regional enstrophy and block intensity as a measure of Kolmogorov entropy. *Atmosphere*, 8(12), 237. https://doi.org/10.3390/atmos8120237.

Kalnay, E., Kanamitsu, M., Kistler, R., Collins, W., Deaven, D., Gandin, L., Iredell, M., Saha, S., White, G., Woollen, J., Zhu, Y., Leetmaa, A., Reynolds, R., Chelliah, M., Ebisuzaki, W., Higgins, W., Janowiak, J., Mo, K.C., Ropelewski, C., Wang, J., Jenne, R. and Joseph, D. (1996) The NCEP/NCAR 40-year reanalysis project. *Bulletin of the American Meteorological Society*, 77, 437–471.

Lau, W.K.M. and Kim, K.-M. (2012) The 2010 Pakistan flood and Russian heat wave: teleconnection of hydrometeorological extremes. *Journal of Hydrometeorology*, 13, 392–403. https://doi.org/10.1175/JHM-D-11-016.1.

Lejenäs, H. and Økland, H. (1983) Characteristics of northern hemisphere blocking as determined from a long time series of observational data. *Tellus A*, 35(5), 350–362. https://doi.org/10.3402/tellusa.v35i5.11446.

Lupo, A.R. and Smith, P.J. (1995) Climatological features of blocking anticyclones in the northern hemisphere. *Tellus A*, 47(4), 439–456. https://doi.org/10.1034/j.1600-0870.1995.t01-3-00004.x.

Lupo, A.R., Mokhov, I.I., Akperov, M.G., Chernokulsky, A.V. and Hussain, A. (2012) A dynamic analysis of the role of the planetary and synoptic scale in the summer of 2010 blocking episodes over the European part of Russia. *Advances in Meteteorology*, 2012, 584257 11 pages.

Lupo, A.R., Jensen, A.D., Mokhov, I.I., Timazhev, A.V., Eichler, T. and Efe, B. (2019) Changes in global blocking character during the most recent decades. *Atmosphere*, 10, 00092, 19 pages. https://doi.org/10.3390/atmos10020092.

Luo, D., Yao, Y., Dai, A. and Feldstein, S.B. (2015) The positive North Atlantic oscillation with downstream blocking and Middle East snowstorms: the large-scale environment. *Journal of Climate*, 28, 6398–6418. https://doi.org/10.1175/JCLI-D-15-0184.1.

Mokhov, I.I., Timazhev, A.V. and Lupo, A.R. (2014) Changes in atmospheric blocking characteristics within euro-Atlantic region and northern hemisphere as a whole in the 21st century from model simulations using RCP anthropogenic scenarios. *Global and Planetary Change*, 122, 265–270. https://doi.org/10.1016/j.gloplacha.2014.09.004.

Nunes, M.J., Lupo, A.R., Lebedeva, M.G., Chendev, Y.G. and Solovyov, A.B. (2017) The occurrence of extreme monthly

temperatures and precipitation in two global regions. *Papers in Applied Geography*, 3(2), 143–156. https://doi.org/10.1080/23754931.2017.1286253.

Pavan, V., Tibaldi, S. and Brankovic, C. (2000) Seasonal prediction of blocking frequency: results from winter ensemble experiments. *Quarterly Journal of Royal Meteorological Society*, 141, 2125–2142. https://doi.org/10.1002/qj.49712656708.

Pearson, K. (1896) Mathematical contributions to the theory of evolution. XIX. Second supplement to a memoir on skew variation. *hical Transactions of the Royal Society of London. Series A*, 187, 253–318.

R Core Team. (2018) *R: a language and environment for statistical computing*. R Foundation for Statistical Computing, Vienna, Austria. Available at: https://www.R-project.org/ [Accessed 20th May 2019].

Radcliffe, R.A.S. (1985) Review of spring 1985 over the northern hemisphere. *Weather*, 40, 254–255. https://doi.org/10.1002/j.1477-8696.1985.tb06888.x.

Rimbu, N., Stefan, S. and Necula, C. (2014) The variability of winter high temperature extremes in Romania and its relationship with large-scale atmospheric circulation. *Theoretical and Applied Climatology*, 121, 121–130. https://doi.org/10.1007/s00704-014-1219-7.

Scherrer, S.C., Croci-Maspoli, M., Schwierz, C. and Appenzeller, C. (2006) Two-dimensional indices of atmospheric blocking and their statistical relationship with winter climate patterns in the euro-Atlantic region. *International Journal of Climatology*, 26(2), 233–249. https://doi.org/10.1002/joc.1250.

Shabbar, A., Huang, J. and Higuchi, K. (2001) The relationship between the wintertime North Atlantic oscillation and blocking episodes in the North Atlantic. *International Journal of Climatology*, 21(3), 355–369. https://doi.org/10.1002/joc.612.

Sillmann, J., Croci-Maspoli, M., Kallache, M. and Katz, R.W. (2011) Extreme cold winter temperatures in Europe under the influence of North Atlantic atmospheric blocking. *Journal of Climate*, 24(22), 5899–5913. https://doi.org/10.1175/2011JCLI4075.1.

Sitnov, S.A., Mokhov, I.I. and Lupo, A.R. (2014) Evolution of the water vapor plume over Eastern Europe during summer 2010 atmospheric blocking. *Advances in Meteorology*, 2014, 253953–253911. https://doi.org/10.1155/2014/253953.

Sitnov, S.A., Mokhov, I.I. and Lupo, A.R. (2017) Ozone, water vapor, and temperature anomalies associated with atmospheric blocking events over Eastern Europe in spring - summer 2010. *Atmospheric Environment*, 164, 180–194. https://doi.org/10.1016/j.atmosenv.2017.06.004.

Sousa, P.M., Trigo, R.M., Barriopedro, D., Soares, P.M.M., Ramos, A.M. and Liberato, M.L.R. (2016) Responses of European precipitation distributions and regimes to different blocking locations. *Climate Dynamics*, 48, 1141–1160. https://doi.org/10.1007/s00382-016-3132-5.

Sousa, P.M., Trigo, R.M., Barriopedro, D., Soares, P.M.M. and Santos, J.A. (2017) European temperature responses to blocking and ridge regional patterns. *Climate Dynamics*, 50, 457–477. https://doi.org/10.1007/s00382-017-3620-2.

Tayanç, M., Karaca, M. and Dalfes, H.N. (1998) March 1987 cyclone (blizzard) over the eastern Mediterranean and Balkan region associated with blocking. *Monthly Weather Review*, 126(11), 3036–3047. https://doi.org/10.1175/1520-0493.

Tibaldi, S. and Molteni, F. (1990) On the operational predictability of blocking. *Tellus A*, 42(3), 343–365.

Tibaldi, S., D'Andrea, F., Tosi, E. and Roeckner, E. (1997) Climatology of northern hemisphere blocking in the ECHAM model. *Climate Dynamics*, 13(9), 649–666. https://doi.org/10.1007/s003820050188.

Treidl, R.A., Birch, E.C. and Sajecki, P. (1981) Blocking action in the northern hemisphere: a climatological study. *Atmosphere-Ocean*, 19(1), 1–23. https://doi.org/10.1080/07055900.1981.9649096.

Türkeş, M. and Erlat, E. (2009) Winter mean temperature variability in Turkey associated with the North Atlantic oscillation. *Meteorology and Atmospheric Physics*, 105(3–4), 211–225. https://doi.org/10.1007/s00703-009-0046-3.

de Vries, H., Woollings, T., Anstey, J., Haarsma, R.J. and Hazeleger, W. (2013) Atmospheric blocking and its relation to jet changes in a future climate. *Climate Dynamics*, 41(9–10), 2643–2654. https://doi.org/10.1007/s00382-013-1699-7.

Weather Log. (2015) September 2015: coolest September for 21 years in south-but a vast improvement on summer in Scotland. *Weather*, 70, 1–5.

Whan, K., Zwiers, F. and Sillmann, J. (2016) The influence of atmospheric blocking on extreme winter minimum temperatures in North America. *Journal of Climate*, 29(12), 4361–4381. https://doi.org/10.1175/JCLI-D-15-0493.1.

Wickham, H. (2016) *ggplot2: Elegant Graphics for Data Analysis*. New York: Springer-Verlag Available at: http://ggplot2.org [Accessed 20th May 2019].

Wickham, H., Francios, R., Henry, L. and Müller, K. (2017). Dplyr: a grammar of data manipulation. Available at: https://cran.r-project.org/package=dplyr [Accessed 20th May 2019].

Wiedenmann, J.M., Lupo, A.R., Mokhov, I.I. and Tikhonova, E.A. (2002) The climatology of blocking anticyclones for the northern and southern hemispheres: block intensity as a diagnostic. *Journal of Climate*, 15(23), 3459–3473. https://doi.org/10.1175/1520-0442.

Yao, Y., Luo, D., Dai, A. and Feldstein, S.B. (2016) The positive North Atlantic oscillation with downstream blocking and Middle East snowstorms: impacts of the North Atlantic jet. *Journal of Climate*, 29, 1853–1876. https://doi.org/10.1175/JCLI-D-15-0350.1.